

## Journal Pre-proof

### Brain Pathology Identification Using Computer Aided Diagnostic Tool: A Systematic Review

Anjan Gudigar , U. Raghavendra , Ajay Hegde , M. Kalyani ,  
Edward J. Ciaccio , U. Rajendra Acharya

PII: S0169-2607(19)31666-9  
DOI: <https://doi.org/10.1016/j.cmpb.2019.105205>  
Reference: COMM 105205



To appear in: *Computer Methods and Programs in Biomedicine*

Received date: 29 September 2019  
Revised date: 12 November 2019  
Accepted date: 12 November 2019

Please cite this article as: Anjan Gudigar , U. Raghavendra , Ajay Hegde , M. Kalyani , Edward J. Ciaccio , U. Rajendra Acharya , Brain Pathology Identification Using Computer Aided Diagnostic Tool: A Systematic Review, *Computer Methods and Programs in Biomedicine* (2019), doi: <https://doi.org/10.1016/j.cmpb.2019.105205>

This is a PDF file of an article that has undergone enhancements after acceptance, such as the addition of a cover page and metadata, and formatting for readability, but it is not yet the definitive version of record. This version will undergo additional copyediting, typesetting and review before it is published in its final form, but we are providing this version to give early visibility of the article. Please note that, during the production process, errors may be discovered which could affect the content, and all legal disclaimers that apply to the journal pertain.

© 2019 Published by Elsevier B.V.

## Highlights

- The state-of-the-art techniques for brain pathology identification (BPI) with two-class and multiclass are analyzed using brain magnetic resonance imaging.
- The detailed investigation of handcrafted feature learning based approach and deep neural network based approach is performed.
- The open issues for further advancement in BPI are discussed.

Journal Pre-proof

# Brain Pathology Identification Using Computer Aided Diagnostic Tool: A Systematic Review

Anjan Gudigar<sup>a</sup>, U Raghavendra<sup>a\*</sup>, Ajay Hegde<sup>b</sup>, Kalyani M<sup>a</sup>, Edward J Ciaccio<sup>c</sup>, U Rajendra Acharya<sup>d,e,f</sup>

<sup>a</sup>Department of Instrumentation and Control Engineering, Manipal Institute of Technology, Manipal Academy of Higher Education, Manipal 576104, India.

<sup>b</sup>Neurosurgery, Institute of Neurological Sciences, NHS Greater Glasgow and Clyde, Glasgow, UK

<sup>c</sup>Department of Medicine, Columbia University Medical Center, New York, USA.

<sup>d</sup>Department of Electronics and Computer Engineering, Ngee Ann Polytechnic, Clementi 599489, Singapore.

<sup>e</sup>Department of Biomedical Engineering, School of Science and Technology, SUSS University, Clementi 599491, Singapore.

<sup>f</sup>International Research Organization for Advanced Science and Technology (IROAST)  
Kumamoto University, Kumamoto, Japan.

\*Corresponding Author

Postal Address: Department of Instrumentation and Control Engineering, Manipal Institute of Technology, Manipal Academy of Higher Education, Manipal 576104, India.

Telephone: (91) 820-2925152; Email Address: Raghavendra U<raghavendra.u@manipal.edu>

## Abstract

Computer aided diagnostic (CAD) has become a significant tool in expanding patient quality-of-life by reducing human errors in diagnosis. CAD can expedite decision-making on complex clinical data automatically. Since brain diseases can be fatal, rapid identification of brain pathology to prolong patient life is an important research topic. Many algorithms have been proposed for efficient brain pathology identification (BPI) over the past decade. Constant refinement of the various image processing algorithms must take place to expand performance of the automatic BPI task. In this paper, a systematic survey of contemporary BPI algorithms using

brain magnetic resonance imaging (MRI) is presented. A summarization of recent literature provides investigators with a helpful synopsis of the domain. Furthermore, to enhance the performance of BPI, future research directions are indicated.

**Keywords:** Brain pathology, Computer aided diagnostic, Classification, Deep learning, Feature extraction, Magnetic resonance imaging

## 1. Introduction

The human brain is the seat of higher learning and computation. Often referred to as the central processing unit of a human being, the brain is affected by more than 600 different diseases including brain tumours, epilepsy, dementia, cerebrovascular diseases, infections, and trauma. The World Health Organisation estimates that neurological disorders affect up to one billion people worldwide, and remain one of the most disabling diseases of mankind, causing an estimated 16.8% of deaths annually [1].

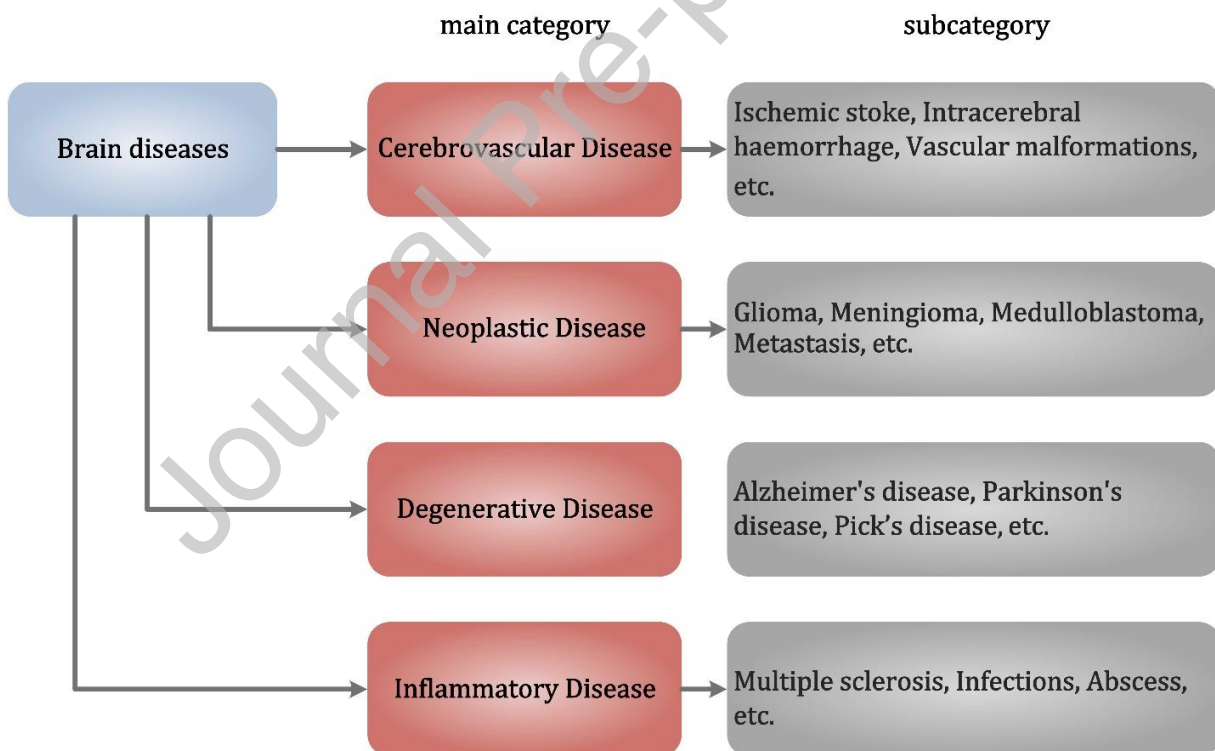


**Figure 1:** General categories of brain diseases.

Neurological disorders are typically devastating to affected patients and their families, often depriving the patient of satisfactory quality-of-life. A rapid and timely diagnosis of these diseases can therefore significantly improve a patient's life.

Neurological disorders occur over a broad spectrum, from degenerative diseases like Alzheimer's disease, Parkinson's disease, vascular disorders such as stroke, intracerebral haemorrhage, vascular malformations, neoplastic ailments which range from benign brain tumours to life-threatening malignant cancers, and inflammatory disorders which include a variety of infections. The various brain diseases are outlined in [Figure 1](#). Each of these clinical conditions is diagnosed by radiological imaging, and the value of this tool is unprecedented. Imaging modalities are not only helpful in the diagnosis of new disease, but they also form a very important role in the follow-up of many neurological diseases. Due to the high volume and complexity of the imaging data, it is difficult for experts to assimilate and analyse large volumes of data for diagnosis and treatment [2]. The diagnosis is time-consuming, error prone, and diagnosticians are subject to fatigue. Automation in the field of neuroimaging may be useful to remedy several of these problems; it could: a) increase accuracy and precision when analyzing images [3] b) minimize interobserver variability [4] and c) enhance speed of image analysis and reporting [5,6]. These problems are particularly relevant to large populous countries including India and China, where computational methods have made faster inroads to Tier 2 and 3 cities in comparison to the presence of radiologists [7]. Thus, medical analytics require development of automated decision systems, which can be done by utilizing computational intelligence for fast, accurate, and efficient diagnosis [8], prognosis, and treatment of neurological illness [2].

In the modern era, the computer aided diagnostic (CAD) tool has undergone tremendous development. It is designed to monitor the health condition of patients at anytime and anywhere, with the help of wireless networks [9]. CAD comprises a dedicated computer system for interpreting medical images, thereby serving the radiologist or other doctors to provide second opinions (please refer to [Figure 2](#)). CAD systems and technology can enhance the diagnostic accuracy of radiologists, reduce workload, decrease missing of pathologies due to fatigue, and boost the inter and intra reader variability. Since radiologists are the final decision-makers, the collaborative effort between radiologists and computer with a CAD tool amplifies the diagnostic

ability. On the other hand, CAD systems must be equipped by radiologists in areas such as ability to learn and recognize brain diseases. Hence, the development of the CAD system using pattern recognition techniques together with machine learning algorithms plays a key role. Any such algorithms can be applied to process large datasets when properly implemented. Parallel execution of these algorithms can help to accelerate the entire process.

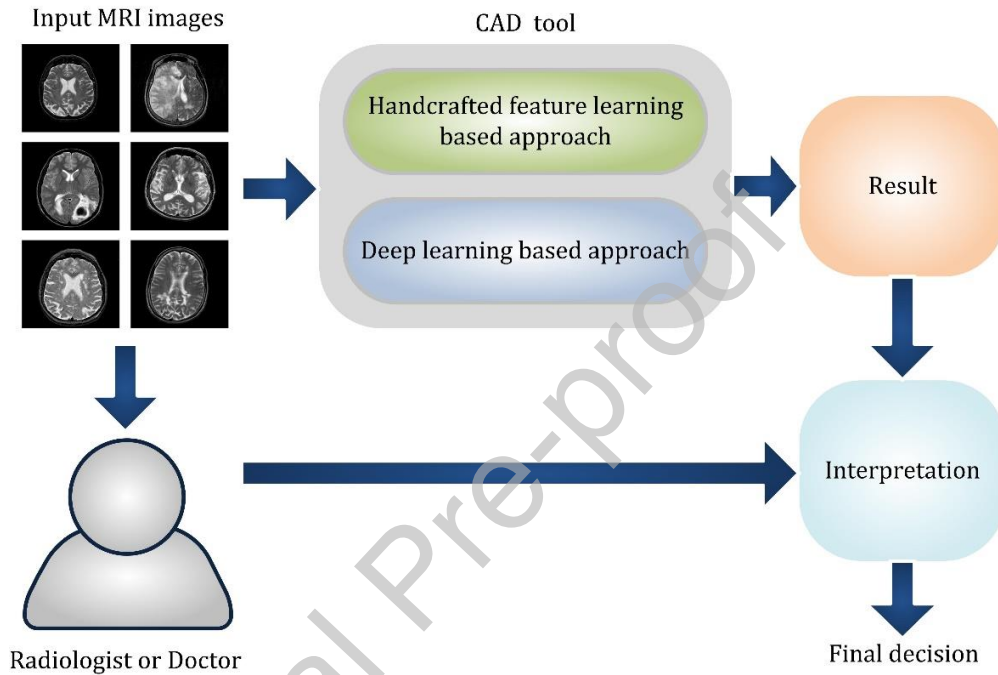


Figure 2: General structure of the diagnostic system.

In general, the evaluation of brain pathology is done using two types of CAD systems: i) a system that categorizes normal and pathological brain by treating the problem as a two-class or multiclass problem, and ii) a system that distinguishes the lesions. CAD is the integration of several image processing algorithms which includes preprocessing, segmentation, feature extraction, dimensionality reduction, and classification. Many different techniques are used to develop a CAD tool and various techniques are presented in [10-14, 113]. The cost of categorizing a pathological brain as healthy due to some technical flaw in CAD is severe because the patients may forgo treatment, which is unacceptable. To rectify, more recent work has been concentrated on constructing datasets with more diseased or pathological brain imagery as compared to input of normal or healthy brain images. This is to make the classifier more precise

towards predicting the diseased brain. Hence, the main focus of this paper is to present a critical review of CAD tools useful to identify brain pathology.

The primary focus of this paper is to provide an overview of artificial intelligence techniques that are useful with holistic features for diagnosis of brain pathology. Furthermore, we address the methodological exertions made by researchers in order to enhance the performance of CAD tools for brain pathology identification (BPI). Finally, open issues for the future development of BPI are discussed as possible avenues of research. The remainder of this paper is organized as follows: Section 2 addresses imaging modalities and public datasets. The complete structure of a state-of-the-art CAD model is delineated in Section 3. Section 4 presents discussion and analysis of best performing CAD tools. Finally, this paper concludes in Section 5.

## 2. Brain imaging modalities and available datasets

In recent years, advancing imaging techniques have altered the landscape in the diagnosis of complex neurological diseases. The progress in technology has enabled the use of safe imaging techniques in hospitals worldwide. Medical doctors and scientific researchers can analyze brain activity and complications using imaging techniques. Computed tomography (CT) and magnetic resonance imaging (MRI) are the two main technologies which have increased precision in the diagnosis and management across the spectrum of neurological disorders. The former utilizes X-rays for cross-sectional imaging [15]. The later uses a magnetic field to reorient hydrogen ions in water molecules and render high-quality imagery of biological structures [16]. These techniques are assistive to understand brain structure without need for invasive neurosurgery. In addition, positron emission tomography (PET) can provide exquisite information to study brain tissues. [Figure 3](#) depicts brain anatomy using various imaging modalities<sup>1</sup>.

---

<sup>1</sup> <http://www.med.harvard.edu/aanlib/hms1.html>

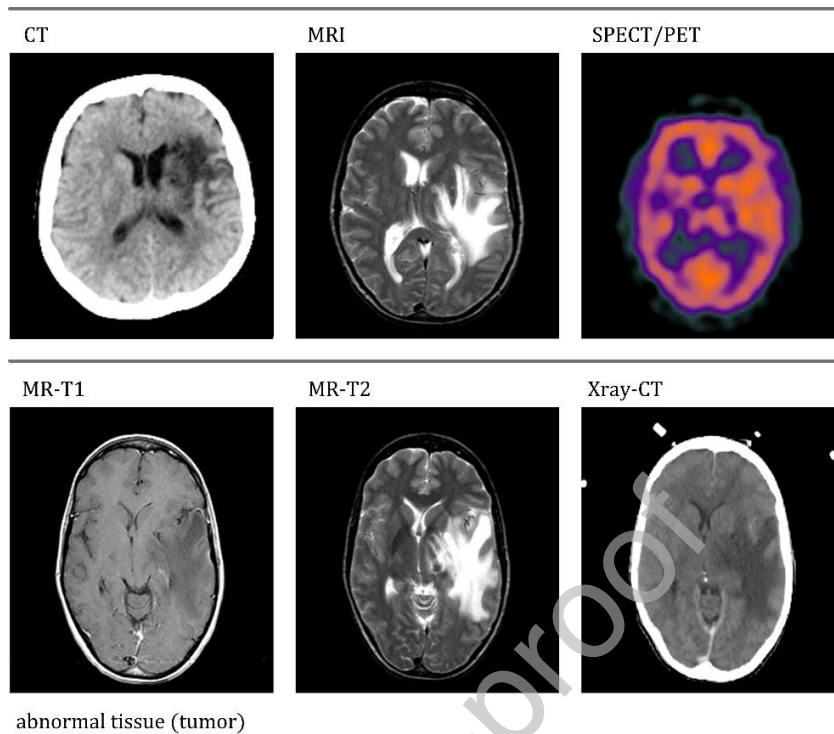


Figure 3: Sample images of various imaging modalities.

Among these techniques, MRI is efficient, as it provides high contrast of soft tissues, and does not emit any ionizing radiation. MRI scanners are particularly well suited to image the non-bony parts or soft tissues of the body. The brain, spinal cord, and nerves, as well as muscles, ligaments, and tendons, are clearly observable with MRI as compared with standard X-rays or CT [17]. Primarily, the MRI signal depends on the three parameters: density of protons, and T1 and T2 relaxation times. T1 and T2 are influenced by tissue rigidity and are responsible for divergence among soft tissues [11]. Often, T1- and T2- weighted imagery is useful for demonstrating the anatomy and pathology of brain, respectively (please refer to Figure 3, which depicts abnormal tissue in various scans). Since MRI produces rich information of various types of tissues, it has evolved as a widespread imaging modality in recent years. Due to its attractive features, it can be suitably used in the development of CAD tools.

In order to develop a CAD tool to identify brain pathology, many datasets are publicly available. These databases are useful for the evaluation of diagnostic algorithms for characterization of brain abnormality. The dataset of Harvard Medical School<sup>2</sup> is widely used for

<sup>2</sup> <http://www.med.harvard.edu/aanlib/>



identification of brain abnormality. Other datasets such as the open access series of imaging studies (OASIS)<sup>3</sup> and brain tumor image segmentation (BRATS)<sup>4</sup> are also used for specific disease analysis, such as for analysis of Alzheimer's disease and brain tumors, respectively.

***Harvard Medical School dataset:***

This dataset provides four classes of major brain diseases viz.: cerebrovascular, neoplastic, infectious, and degenerative. The investigators have developed different datasets for the design of the CAD tool. The datasets are labeled: Dataset1, Dataset2, Dataset3, Dataset4, and Dataset5, and are used with different normal and abnormal count i.e.:  $DS - total = normal + abnormal$   
Thus: DS1-66 (18+48), DS2-160(20+140), DS3-255(35+220), DS4-612(83+529), DS5: with different normal and abnormal count. All dataset images are of dimension  $256 \times 256$  and were acquired along the axial plane using the T2-weighted MRI mode. Diseases such as glioma, meningioma, sarcoma, Alzheimer's disease, Alzheimer's disease plus visual agnosia, Pick's disease, Huntington's disease, chronic subdural hematoma, cerebral toxoplasmosis, etc., are included in the abnormal class. In Dataset4, an extra thirteen abnormalities were added for comparison with Dataset3. Figure 4 depicts normal and various abnormal MRIs used in CAD tool development. The Harvard Medical School dataset comprises all types of brain abnormalities. The work based on this dataset is discussed in the subsequent sections.

---

<sup>3</sup> <https://www.oasis-brains.org/>

<sup>4</sup> <https://www.smir.ch/BRATS/Start2015>

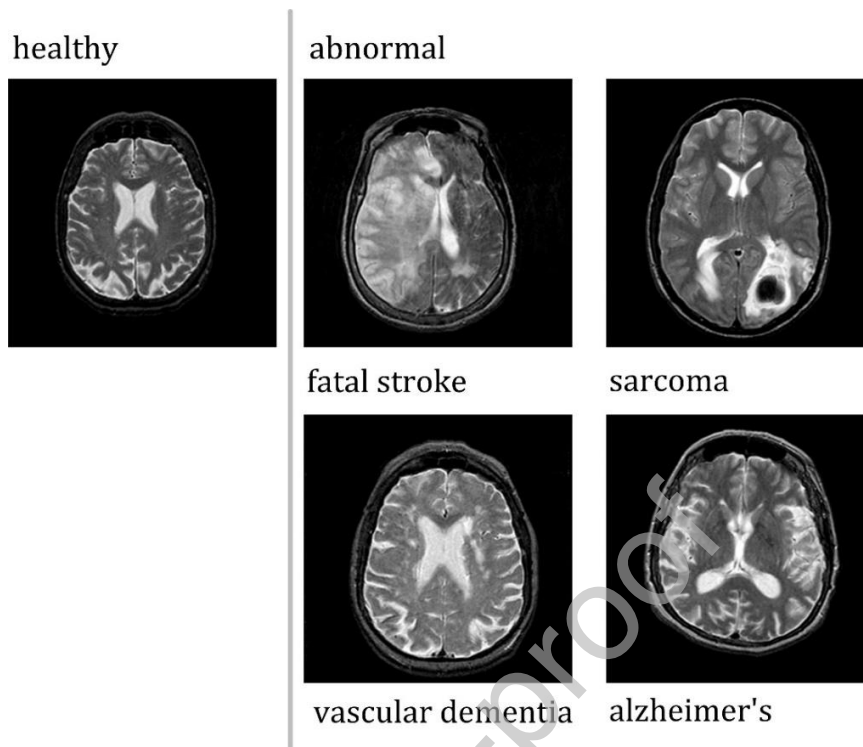


Figure 4: Sample MRI-T2 images from Harvard Medical School.

### 3. Generic methodology for CAD tool using MRI

The development of CAD tools can assist medical doctors in diagnosis, prognosis, and pre-and post-surgical processes, depending on whether the subject is healthy or suffering from brain disorder such as sarcoma, Pick's disease, etc. The detailing obtained in the MRI brain imagery can be utilized to build a CAD tool with the help of image processing algorithms. Since manual interpretation of MRIs from a huge repository is a difficult task, this necessitates the development of such automated tools.

In general, two approaches are employed to develop a CAD tool for BPI, described as follows:

#### *Handcrafted feature learning based approach*

Generally, this methodology comprises the following steps: 1) preprocessing, 2) feature extraction, 3) dimensionality reduction, 4) feature ranking, and 5) classification. Preprocessing is

the initial stage used to boost the feature robustness and classification accuracy of the BPI system [109]. Using the second, third, and fourth step, suitable features are generated to characterize brain imagery. These features are further independently used by the classifiers to categorize normal and pathological brain MRIs. The most commonly used steps are feature extraction, dimensionality reduction, and classification. Other steps, such as preprocessing and feature ranking, are optional, and integrated by the research community to enhance system performance. The detailed descriptions of these steps are described in the subsequent section. The taxonomy of the general architectural flow using a handcrafted feature learning approach for BPI is provided in Figure 5.

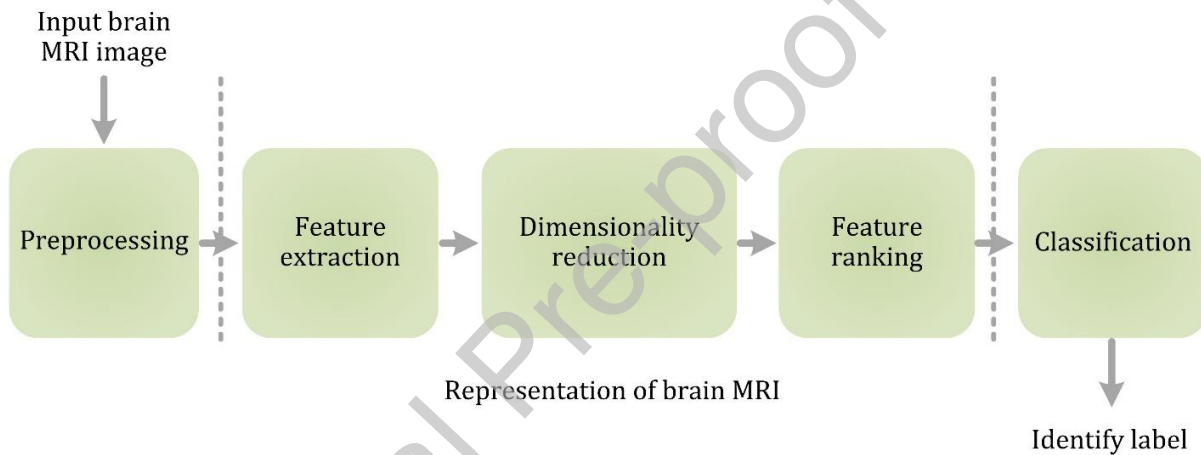


Figure 5: General block diagram using handcrafted feature learning approach

### ***Deep neural network based approach***

The deep learning (DL) approach, such as via the convolutional neural network (CNN), stacks the numerous convolutional and max-pooling or sub-sampling layers successively. Each layer only accepts connections from its preceding layer. It extracts the features hierarchically by mapping the raw pixel intensities of an image to feature vectors, with subsequent classification via the fully connected layers [18,19]. The CNNs are followed by a max-pool or average pooling layer to remove redundant information and to reduce the size of the feature map (please refer to Figure 6). The various adjustable parameters are tuned optimally to reduce the misclassification error. Recently, it has become a revolutionary technique for pattern recognition and object classification.

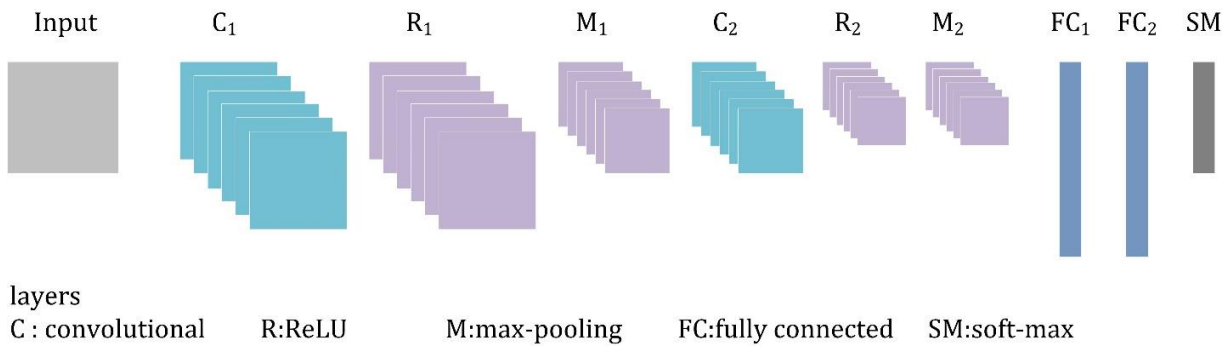


Figure 6: General CNN architecture.

However in order to learn data coding efficiently in an unsupervised manner, the autoencoder (AE) is used [101,102]. It is a type of artificial neural network, and its architecture is shown in Figure 7. One or more encoders and decoders are grouped to establish a convolutional AE; in this study the encoder includes convolutional and pooling layers and the corresponding decoder includes unpooling and deconvolution layers [103]. In [101], the authors have shown that deep spatial autoencoding models can be proficiently used to capture normal anatomical variability of MRI brain images. The use of convolutional AE is done in [104] to segment the brain lesion accurately.

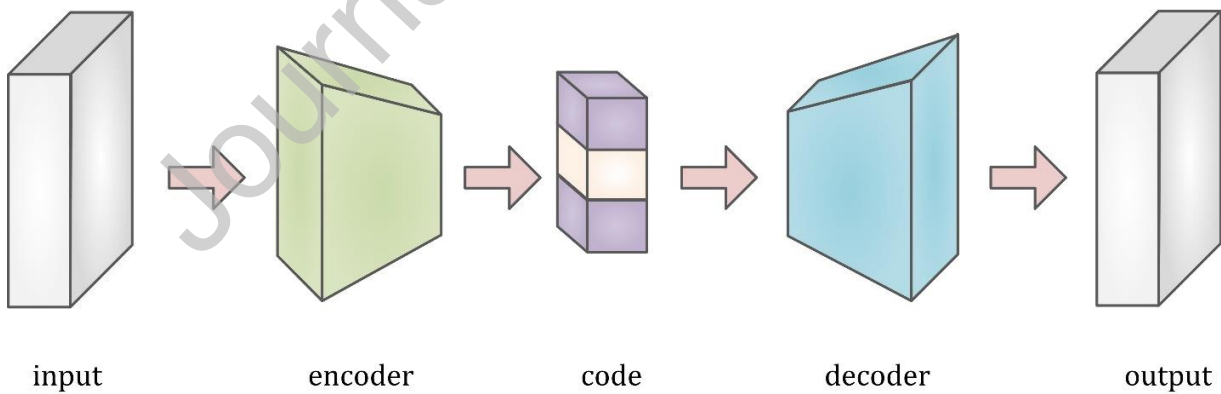


Figure 7: Basic structure of an autoencoder.

### 3.1.Preprocessing

In this stage, the significant brain region can be extracted and enhanced from imagery by removing skull tissue or extra cranial tissue features. The skull tissue imagery features can be removed with assistance from morphological operations [20]. De-noising techniques include the median [21, 22] and Wiener filters [23]. Contrast limited adaptive histogram equalization (CLAHE) is a common technique for improving image quality [24-29]. Furthermore, the region of interest (ROI) can be extracted via K-means clustering [30] and a pulse coupled neural network (PCNN) [31]. Since PCNN is used for edge extraction and image segmentation, its modification such as feedback PCNN (FPCNN) [21, 32] and simplified PCNN (SPCNN) [33] are used for ROI extraction.

### 3.2.Feature extraction

Various features have been described to characterize brain MRI in prior works. The feature design technique is mainly developed to address nonlinearities in brain structure. Different investigators have designed efficient features to address the BPI problem. The most popular feature choices are computed using the following two approaches:

- I. Employ transformation or decomposition techniques, then use the resultant raw coefficients as primary features.
- II. Use raw coefficients, then compute descriptors as primary features.

In the first approach, the discrete wavelet transform (DWT) [22, 23, 32, 34-46] is utilized most often. Apart from this, the Gabor wavelet [47], the Ripplelet transform Type-I (RT) [48], weighted-type fractional Fourier transform (WFRFT) [49], stationary wavelet transform (SWT) [50], orthogonal discrete Ripplelet-II transform (O-DR2T)[26], DR2T [27], and fast discrete curvelet transform (FDCT) [24, 25, 33, 51] are useful for feature extraction.

In the second approach, the descriptors include: entropy, energy, and skewness. In [52,53], a histogram of intensities was calculated, then the improved orthogonal DWT i.e., Slantlet transform (ST) is applied to extract lesser relevant features. The features are extracted via the gray level co-occurrence matrix (GLCM) using the method of Haralick et al. [54] to analyze texture [20, 55, 56]. For improved performance, investigators have modeled wavelet coefficients using generalized autoregressive conditional heteroscedasticity (GARCH) [57]. The entropy can be implemented to portray image texture, as it can detect randomness. Hence, many research

studies have used this statistical measure to quantify texture. In [58], a spider web plot is constructed using wavelet entropy, and the calculated area is utilized as the primary feature set. The triplets (Shannon entropy, variance, and energy) [59] and entropies [60] are extracted from the DWT. The Tsallis entropy is also computed over the coefficients of the wavelet packet transform (WPT) [61, 62]. Likewise, the entropy was computed based on the spectra of the fractional Fourier transform (FRFT) [63, 64]. Moreover, the dual-tree complex wavelet transform (DTCWT) is employed to recover directional selectivity, and variance and entropy (VE) are extracted for each direction and decomposition level [65]. The authors have achieved a promising result, as DTCWT can detect edges independent of their angle, in contrast to the DWT. In [66], fractal dimensions are estimated using the Minkowski-Bouligand dimension (MBD) technique. The extracted MBD features for various box sizes represent the global feature vector. In order to decompose the image at different orientations and scales, the curvelet transform has been used. For simplicity and reduced redundancy, its next generation i.e. the fast discrete curvelet transform (FDCT) is incorporated in CAD tools. The features are derived using entropy over sub-bands of curvelet, and the obtained textural features are termed as FCEntF [67]. In [29], a comparison of various multiresolution analyses is performed. It is also observed that the combination of shearlet transform and textural features have achieved better classification accuracy. They have used GLCM based as well as run-length matrix based features for the identification of abnormal brain MRIs. Recently, brain imagery has been decomposed using variational mode decomposition (VMD) and bidimensional empirical mode decomposition (BEMD) [68]. Figure 8 shows the result of various methods to represent brain. The bispectral features and entropies are extracted over each coefficient of the resultant decomposition. It is noted that VMD with higher order spectra (HOS) can handle both the two-class and multiclass scenario effectively. The coefficients of HOS cumulants are very efficient to represent the subtle changes in the brain MRIs (please refer to Figure 9). The features derived from these coefficients do not rely on the segmentation and detection algorithms.



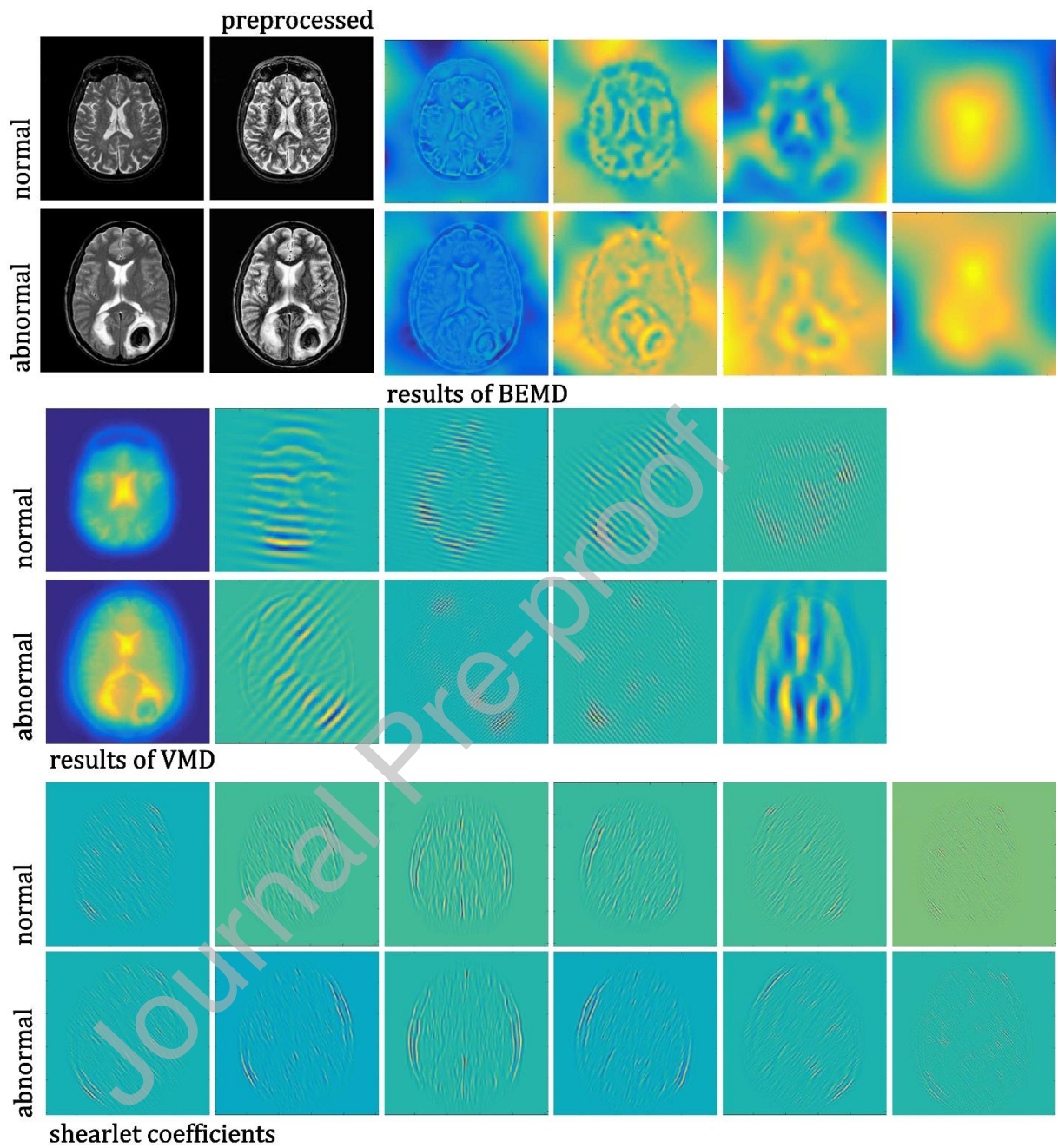
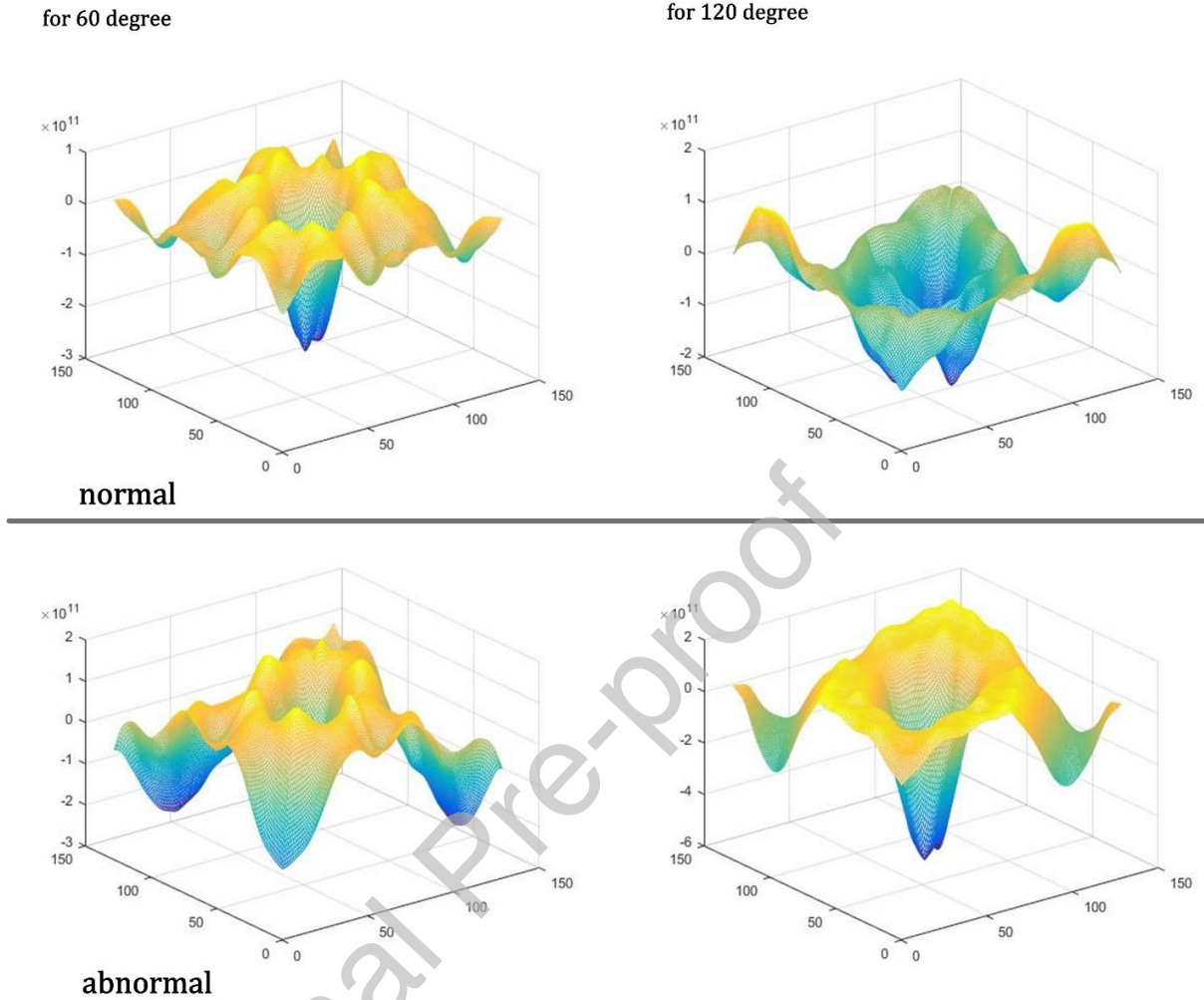


Figure 8: BEMD, VMD, and shearlet coefficients of normal and abnormal brain MRI images.



**Figure 9:** The coefficients of third order HOS cumulants for normal and abnormal MRI images.

Apart from these features, the authors have used: two-dimensional PCA (2DPCA) [28], intensity of brain MRIs [56], Hu moment invariant [60], eigenbrains [69], scale invariant feature transform and histogram of oriented gradient [70], and pseudo Zernike moment [71]. These features have shown comparable performances for smaller datasets.

### 3.3. Dimensionality reduction

The main purpose of a dimensionality reduction technique is to preserve the most salient information of the data points, while projecting from a high dimensional to a lower dimensional space. Generally, dimensionality reduction can be categorized into subspace learning [72] and



feature selection methods [73]. These techniques extract useful information from the created feature space.

Principal component analysis (PCA) and linear discriminant analysis (LDA) are classical subspace learning methods, and have a proven efficacy in many pattern recognition problems. PCA [24-28, 30, 32, 33, 35-44, 46, 48-51, 55, 57, 74] and LDA [24-28, 33, 44, 55, 57] are extensively used to reduce redundant information in feature representation. In addition, the probabilistic PCA (PPCA) is also used [23, 45]. Since the BPI possesses a highly non-linear data point, the graph embedding technique i.e., supervised neighborhood projection embedding (SNPE) is proposed in [68]. These methods are motivated by subspace learning on the graph, by finding the graph and its corresponding weighting matrix [75]. This preserves the topological structure of vertices in the graph, and is able to produce the optimal class separation. Graph embedding ensures that the neighboring data points in the original space are closely situated in the reduced space. Occasionally, the authors have also used particle swarm optimization (PSO) [20, 29] and normalized mutual information feature selection (NMIFS) [76] to select significant features.

### 3.4.Feature ranking

It is one of the important stages utilized to arrange the features based on score. The higher the score, the more discriminative is the feature. The class distinguishability of the feature vectors is computed using statistical tests such as Wilcoxon [56], Welch's t-test (WTT) [63], analysis of variance (ANOVA) [68] and Kruskal-Wallis [77].

### 3.5.Classification

This stage is focused to make a clinical decision on a pathology of brain or multiple classes of it, by discerning patterns corresponding to classes. Factors such as computational resource and classification accuracy are considered to select suitable classifiers. From Table 1 it is evident that the appropriate categorization of brain MRI images is possible using supervised techniques, such as the extreme learning machine (ELM) [25,67], random forest (RF) [45,46], back propagation neural network (BPNN) [56] and the support vector machine (SVM) [68]. These classifiers are only highlighted due to their efficacy in classifying two- and multiclass scenarios with sufficient numbers of brain MRI training images.

The RF metric is a collection of tree-structured classifiers [78], and it is combined with the AdaBoost (ADBRF) classifier to improve stability and accuracy [45]. For generalization and fast learning capability, ELM was developed [79]. Furthermore, the kernel technique can be applied to ELM to achieve improved performance. The Kernel ELM (KELM) involves a kernel parameter and regularization parameter, which require proper tuning to achieve better generalization capability. Hence, during training, the validation set is employed to identify the optimal KELM parameters [67]. In BPNN, optimal selection of the number of neurons in the hidden layer is a vital issue. A network with lesser or a surplus amount of hidden neurons may introduce ambiguity and lead to poor generalization. Hence, a Bayesian regularization algorithm can be useful to overcome the overfitting issue of neural networks [56, 80]. Much work has employed SVM [81] and its variants i.e., least squares SVM (LS-SVM) [48], generalized eigenvalue proximal SVM (GEPSVM) [50], fuzzy SVM (FSVM) [61], and twin SVM (TSVM) [63], to achieve promising results. Herein, the maximum margin of the hyperplane is defined by the data points known as *support vectors*. The multiclass categorization is performed by employing a one-against-all strategy using binary SVMs. SVM classification is highly accurate, fast, and less susceptible to overfitting, in comparison with other classification methods. Hence, the work in [68] outperformed using SVM with a polynomial kernel. It is also noted that PSO combined with ELM [24] and SVM [29, 42] can achieve comparable accuracy. Many experiments with various datasets are carried out with combinations of classifiers i.e., use of self-organizing hierarchical PSO (HPSO) [24], sine cosine algorithm (SCA) [25], modified PSO (MPSO) [27], modified differential evolution (MDE) [28], adaptive chaotic PSO (ACPSO) [36], scaled chaotic artificial bee colony (SCABC) [40], genetic pattern search (GPS) [43], PSO with time-varying acceleration-coefficient (PSOTVAC) and Winner-Takes-All (WTA) [59], adaptive real-coded biogeography-based optimization (ARCBBO) [64], BBO [82], and quantum-behaved PSO (QPSO) [83]. However, such classifiers can predict test images suitably only if the nonlinearity of extracted features is correctly addressed in the preceding stage. Figure 10 shows the best performance of these classifiers for a sample size of 200 or greater.

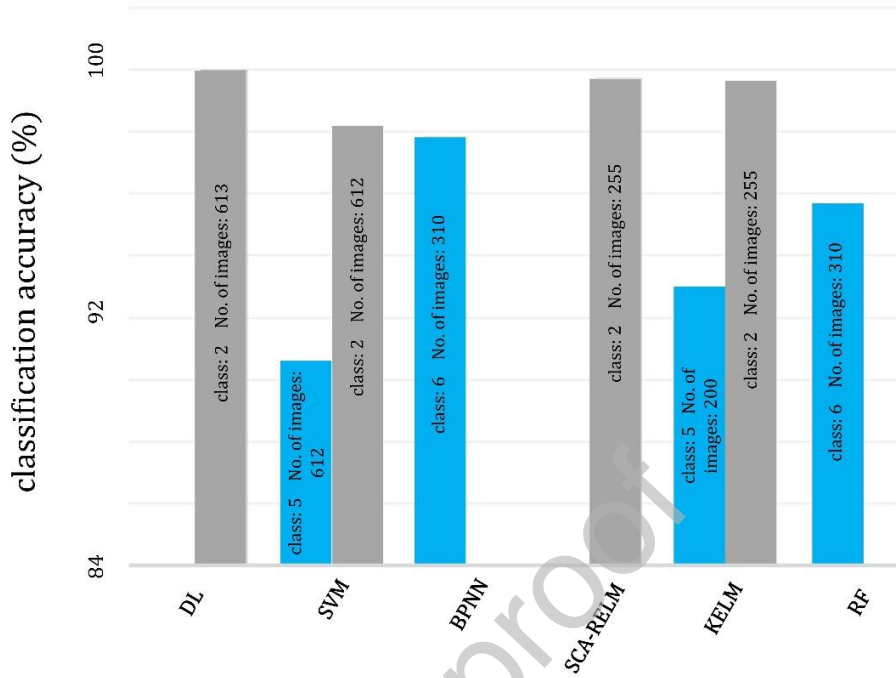


Figure 10: Accuracy levels achieved by various classifiers with a sample size of 200 or greater.

The DL techniques such as AlexNet [84] and ResNet-34 [85] are used to learn the feature representation of brain MRIs automatically. These algorithms pool feature extraction and classification into an integrated neural network. It is observed that the ResNet-34 model achieved the highest classification accuracy of 100% for the two class problem. The problems such as face recognition, traffic sign recognition, etc. have thousands of images for training and testing. However, BPI datasets often contain only a few hundred images. Hence, it is not practical to partition these datasets into train and test sets. More often, a cross-validation scheme is adopted to show the robustness of the system. Moreover, various parameters such as accuracy: Acc(%), sensitivity: Sen(%), and specificity: Spe(%) are computed to decide whether or not the developed system is competent.

In the following section, feature extraction, dimensionality reduction, and classification techniques are reviewed, and their performances are compared in the form of a table (please refer to Table 1).

Table 1: Comparison of work conducted to identify brain pathology.

Ref.No	DATASET DESCRIPTION	PRE PROCESSING/ROI SEGMENTATION	FEATURE EXTRACTION	FEATURE REDUCTION/ SELECTION	CLASSIFICATION	RESULT (Accuracy: Acc(%), Sensitivity: Sen(%), Specificity: Spe(%))			
						DEEP NEURAL NETWORK			
						DS4-612/ DS5	DS1-66	DS2-160	DS3-255
2019									
34	Resampled normal: 114  Abnormal: 177		AlexNet + transfer learning			Acc:100  Sen-100  Spe-100			
35	Total:613		Convolutional neural network (CNN) based ResNet-34 model			Acc:100			
39	Normal: 83  Abnormal: 529	CLAHE	Shearlet transform + Texture	PSO	SVM	Acc: 97.38			
38	Normal: 83  Abnormal: 529		VMD + bispectral  feature	SNPE+ ANOVA	SVM:P3	Acc:98.20  Acc:90.68  Sen:99.43  Spe:89.95  <b>Class=5</b>			
36	Total:310		Energy of wavelet sub bands+ textural features of gray level co-occurrence matrix+ intensity		BPNN	Acc: 97.81  <b>Class:6</b>			
05			Local binary pattern and		BPNN	Acc: 85.01			Acc: 94.67

			steerable pyramid					
10	Total: 1074		Deep Transfer Learning (ResNet-50)			Acc: 95.23±		
						0.6		
						<b>Class:5</b>		
2018								
15		CLAHE	FDCT-USFFT	PCA+LDA	SCA-regularized ELM	Acc:100	Acc:100	Acc:99.73
16	Normal:18 Abnormal:107		Wavelet-entropy		KELM	Acc:97.04		
						Sen-97.48		
						Spe-94.44		
16		CLAHE	O-DR2T	PCA+LDA	Improved Jaya algorithm and ELM	Acc:100	Acc:100	Acc:99.69
17		CLAHE	DR2T	PCA+LDA	MPSO-ELM	Acc:100	Acc:100	Acc:99.69
12	Normal:5 Abnormal:85	Median Filter	DWT	PCA	QDA (i.e., quadratic discriminate analysis)	Acc:98.9		
17	Normal:40 Abnormal:160		FCentF-II		K-ELM	Acc:100	Acc:100	Acc:100
						Acc: 93		Acc: 99.65
						<b>Class:5</b>		
18		CLAHE	2D PCA	PCA+LDA	MDE-ELM	Acc:100	Acc:100	Acc:99.65

1		FDCT	PCA	LS-SVM+RBF	Acc:100	Acc:100	Acc:99.61		
1		pseudo Zernike moment		KSVM	Acc:100	Acc: 99.75 ±0.32	Acc: 99.45 ±0.38		
2017									
4		CLAHE	FDCT-WR	PCA+LDA	IHPSO+ELM	Acc:100	Acc:100	Acc:99.65	
3	Normal:14 Abnormal: 87	CLAHE+Simplified pulse coupled neural network	FDCT	PCA+LDA	PNN (i.e., probabilistic neural network)	Acc:100 Sen:100 Spe:100	Acc:100	Acc:99.12	Acc:98.04
3	Total:90	Noise reduction using Wiener filtering	DWT	PPCA	Random subspace classifier+KNN (i.e., k-nearest neighbors)	Acc:100 Sen:100 Spe:100	Acc:100	Acc:100	Acc:99.20
6	Normal:70 Abnormal:240		DWT	PCA	RF	Acc: 95.70  <b>Class=6</b>			
2016									
6		MBD		SLFN+PSO-TTC	Acc:100	Acc:98.19	Acc:98.08		
2	Normal:5 Abnormal:85	wavelet-energy		BBO-KSVM	Acc:97.78 Sen-98.12 Spe-92.00				
3	Normal:5 Abnormal:85	wavelet-energy		QPSO-KSVM	Acc:98.22 Sen-98.59				

				Spe-92.00			
5		DTCWT + VE		TSVM	Acc:100	Acc:100	Acc:99.57
4		FRFE		KC-MLP+ARCBBO	Acc:100	Acc:99.75	Acc:99.53
5		DWT	PPCA	ADBRF	Acc:100	Acc:100	Acc:99.53
2015							
9	OASIS	3D DWT+triplets	PCA	WTA-SVM+PSOTVAC	Acc:81.5		
	Normal controls :97						
	Mild cognitive impairment: 57						
	Alzheimer's disease :24						
7	Normal:18	DWT and entropy		NB (i.e., Naïve Bayes)	Acc:92.6		
	Abnormal:46				Sen:94.5		
					Spe:91.7		
1		WPT + Tsallis entropy		FSVM	Acc:100	Acc:100	Acc:99.49
4		DWT	PCA+LDA	RF			Acc:99.22
3		FRFE	WTT	TSVM	Acc:100	Acc:100	Acc:99.57
9	Normal:5	WFRFT	PCA	GEPSVM	Acc:99.11		
	Abnormal:85				Sen: 99.53		
					Spe: 92		

50		SWT	PCA	GEPSVM+RBF kernel	Acc:100	Acc:100	Acc:99.41
50		DWT+ Entropy +Hu moment invariants		GEPSVM+RBF kernel	Acc:100	Acc:100	Acc:99.45
52		WPT+Tsallis entropy		GEPSVM+RBF kernel	Acc:100	Acc:100	Acc:99.53
77	Normal:25 Abnormal: 63	BEMD +AR coefficients		LS-SVM+ RBF kernel	Acc:100		
2013							
77	Normal:10 Abnormal:70	DWT+GARCH	PCA+LDA	Both k-NN and SVM	Acc:100		
88		RT-I	PCA	LS-SVM	Acc:100	Acc:100	Acc:99.39
					Sen-100	Sen-100	Sen-97
					Spe-100	Spe-100	Spe-99
82	Normal:5 Abnormal:85	DWT	PCA	PSO-KSVM	Acc:97.78		
					Sen:98.12		
					Spe:92		
83	Normal:40 Abnormal:40	DWT	PCA	GPS-FNN (i.e., forward neural network)	Acc:95.18		
88	Normal:15 Abnormal:60	DWT+ spider web plot		PNN	Acc:100		



						Acc:100 (for normal and degenerative disease) <b>Class=5</b>
2012						
5	Normal:41 Abnormal:79		GLCM	PCA+LDA	Both ANN(i.e., artificial neural network) and k-NN	Acc:100
8	Normal:10 Abnormal:56		Fractal dimension + skewness and kurtosis		BPNN	Acc:91.78
0	Normal:6 Abnormal:54	K- means clustering based coarse image segmentation	WT	PCA	ELM	Acc:more than 94
1			DWT	PCA	KSVM	Acc: 99.38
2	Normal: 14 Abnormal:87	FPCNN	DWT	PCA	BPNN	Acc:99 Sen:100 Spe:92.8
2011						
8			DWT	PCA	BPNN	Acc:100
9	Normal:20 Abnormal:30		DWT	PCA	k-NN	Acc:99

9	OASIS Normal:50 Abnormal:50		Gabor + Haralick		backpropagation network	Acc:97
0			DWT	PCA	FNN+SCABC	Acc:100
4	Normal:5 Abnormal:51		DWT+ first order statistics	PCA	Ensemble of classifiers	Acc: 98(normal)  <b>Class:6</b>
2010						
0	Advanced Medical and Dentist Institute, in Bertam, Pulau Pinang, Malaysia.		WT		SVM	Acc:65
0	Brain tumor image Total:478	Extra cranial tissue removal using morphological operations	Wavelet + first order histogram+GLCM	PSO	Modified CPN	Acc:95.02
6			DWT	PCA	ACPSON+FNN	Acc:98.75
7	Normal:10 Abnormal: 60		DWT	PCA	k-NN	Acc:98.6
2009						
5	Normal:10 Abnormal:60		DWT	PCA	k-NN	Acc:98.6 Sen: 98.4

2008				
3	Normal:39 Abnormal:36 Alzheimer's disease	Intensity histogram +ST	FCM (i.e., fuzzy $c$ -means)	Spe:100 Acc:100
2007				
7	Normal:5 Abnormal:43 Alzheimer's disease From Medical Image Processing Group of University of Pennsylvania.	Gabor wavelet	Mean image SVM with Sigmoid kernel	Acc:100
2006				
4	Normal:6 Abnormal:46	Wavelet	SVM	Acc:98
2	Normal:39 Abnormal:36 Alzheimer's disease	Intensity histogram +ST	BPNN	Acc:100

Number of classes are highlighted for multiclass categorization work.

#### 4. Discussion

Computational algorithms or DL have the potential to revolutionize entire areas of analytical science, including neuroimaging analysis. Given the centrality of neuroimaging in the diagnosis and treatment of neurologic diseases, it may be helpful to improve the ways these diseases are diagnosed and treated. [Table 1](#) shows a comparison of all state-of-the-art approaches for recent years. From the previous related study it is observed that:

1. Most of the research work (approximately 96.5%) have incorporated feature extraction and classification techniques. These methods include DWT, FDCT, the shearlet transform, and VMD, along with textural analysis using various statistical measures. On the other hand, only three work have utilized the DL architecture to obtain promising results.
2. Hybrid classification techniques such as a combination of ranking + classification and optimization + classification have achieved tremendous performances. The very high accuracy achieved was in the range of 98% to 100%.
3. A majority of published work have proposed a solution by considering the problem of BPI as a two-class for a smaller dataset. In recent papers however, the multiclass scenario of BPI is utilized with large dataset and a total number of classes of 5 or 6.

It is a challenging task to distinguish healthy versus pathological brain MRIs, as they may exhibit similar appearance. The non-linearity that exists in the brain data can be analyzed using entropy or GLCM based feature descriptors. The entropy based methods such as DWT+triplets [59], WPT+Tsallis entropy [61, 62], FRFE [63], wavelet entropy (WE) [60, 86], and GLCM based methods such as Wavelet + first order histogram + GLCM [20], as well as Gabor wavelet+Haralick features [89], have shown promising results as compared to wavelet-based methods. In order to represent the 2D singularities, FDCT is used [25, 51, 67]. The authors have shown that the entropies based on FDCT are more efficient [67]. A comparison of wavelet, curvelet, and shearlet transforms on a large database is performed in [29]. The authors concluded that shearlet-based textural analyses are more efficient as compared with wavelet and curvelet features. In order to generalize the system, i.e., to work in both a two-class and multiclass scenario, investigators have developed a system based on bispectral features extracted from VMD coefficients [68]. In addition, they created a graph embedding feature space using SNPE to

understand the structure of brain data. The combination of VMD, bispectrum plot, and SNPE are more significant and are analyzed using ANOVA, as shown in [Tables 2 and 3](#). These features are highly significant ( $p < 0.005$ ). The classical dimension reduction techniques such as PCA and LDA have achieved 100% accuracy for the smaller dataset (please refer to [Table 1](#)). These methods do not consider the manifold structure, where data may possibly be located. Hence, SNPE was proposed for the larger dataset to preserve the manifold structure of each class using labeling information [68]. When five different classes are considered, the generated features are nonlinear and achieve satisfactory performance. However, for normal and abnormal classes, most of the normal features have a higher *mean* as compared to abnormal features. These features are statistically significant and effectively represent the signature of the brain anatomy.

[Table 2: Feature distribution with  \$p\$ -value and  \$F\$ -Value for the multiclass scenario.](#)

Features	Normal		Cerebrovascular		Degenerative		Inflammatory		Neoplastic		$p$ -Value	$F$ -Value
	Mean	SD	Mean	SD	Mean	SD	Mean	SD	Mean	SD		
SNPE2	0.9136	0.0003	0.9146	0.0008	0.9136	0.0007	0.9139	0.0003	0.9138	0.0004	4.51E-46	65.53
SNPE18	0.3154	0.0002	0.3153	0.0003	0.3154	0.0004	0.3151	0.0003	0.3151	0.0004	8.53E-18	23.11
SNPE1	-0.4746	0.0001	-0.4732	0.0017	-0.4733	0.0026	-0.4744	0.0002	-0.4744	0.0002	4.84E-16	20.75
SNPE17	0.0004	0.0002	0.0002	0.0002	0.0003	0.0002	0.0002	0.0002	0.0002	0.0002	5.00E-11	14.12
SNPE26	1.1573	0.0003	1.1571	0.0003	1.1571	0.0002	1.1571	0.0003	1.1573	0.0003	2.86E-09	11.84
SNPE4	0.9913	0.0002	0.9915	0.0004	0.9912	0.0006	0.9914	0.0002	0.9915	0.0004	3.13E-09	11.79
SNPE20	-0.3012	0.0002	-0.3013	0.0003	-0.3014	0.0002	-0.3014	0.0002	-0.3012	0.0002	3.21E-09	11.77
SNPE10	-0.7589	0.0005	-0.7589	0.0005	-0.7585	0.0005	-0.7587	0.0005	-0.7587	0.0004	3.83E-09	11.68
SNPE8	0.5560	0.0001	0.5558	0.0003	0.5557	0.0005	0.5559	0.0002	0.5559	0.0003	1.73E-07	9.54
SNPE13	1.3405	0.0001	1.3406	0.0002	1.3406	0.0001	1.3406	0.0001	1.3405	0.0001	3.31E-07	9.18

[Table 3: Feature distribution with  \$p\$ -value and  \$t\$ -value for the two-class scenario.](#)

Features	Normal	Abnormal
----------	--------	----------

	Mean	SD	Mean	SD	<i>p-Value</i>	<i>t-Value</i>
SNPE17	0.0004	0.0002	0.0002	0.0002	1.08E-12	7.2735
SNPE2	0.9136	0.0003	0.9141	0.0007	1.01E-07	5.3891
SNPE20	-0.3012	0.0002	-0.3013	0.0002	3.54E-07	5.1490
SNPE1	-0.4746	0.0001	-0.4737	0.0017	6.37E-06	4.5534
SNPE8	0.5560	0.0001	0.5558	0.0003	9.83E-05	3.9208
SNPE18	0.3154	0.0002	0.3153	0.0003	2.00E-04	3.7279
SNPE26	1.1573	0.0003	1.1572	0.0003	5.00E-04	3.4914
SNPE14	-0.8585	0.0001	-0.8584	0.0002	9.00E-04	3.3126
SNPE24	0.3524	0.0001	0.3523	0.0002	10.00E-04	3.2852
SNPE13	1.3405	0.0001	1.3406	0.0001	21.00E-04	3.0838

It is evident that investigators should consider the required hardware capabilities and execution time when designing a real-world system. It is observed that graph-based methods can be used to understand the inherent topographies of brain data, and they achieve remarkable accuracies [68]. Table 4 shows the various best-performed methods for a large brain dataset. It is noted from Table 4 that authors have used only 395 features as base features to achieve the highest accuracy.

Table 4: Different methods and performances of features.

References	Method	# base features	#selected significant features	Accuracy
[29]	Wavelet-based	136	10	95.09%
[29]	Curvelet-based	4420	10	95.75%
[29]	Shearlet-based	680	15	97.38%
[68]	BEMD-based	316	28	84.47%
[68]	VMD-based	395	25	98.20%

These methods have the capability to run on lesser configured standalone personal computers (PCs). It is also noted that almost all handcrafted feature techniques require system configuration without the need for graphics processing units (GPUs). These methods adopted powerful feature extraction and classifiers to achieve acceptable results [29, 56, 68]. Many compact discriminative features have emerged during the design of BPI systems, which can be generalized and applied to different pattern recognition problems. The hybridization of the classifier techniques i.e., in combination with optimization techniques such as ACPSO+forward neural network(FNN)[36], FNN+SCABC [40], single-hidden layer feedforward neural-network (SLFN)+PSO-TTC [66], BBO+KSVM [82], QPSO+KSVM [83], Kappa coefficient (KC)-multi-layer perceptron (MLP)+ARCBBO [64], IHPSO-ELM (i.e., pooling of self-organizing hierarchical PSO (HPSO) and ELM) [24], MPSO-ELM [27], etc., can be avoided using powerful compact features. Hence, a supervised classification technique can be used alone with a validation scheme. It is also noted that many works have restricted themselves to three datasets i.e., DS1-66, DS2-160, and DS3-255 (please refer to Table 1), and it is difficult to develop a prototype using these methods.

In DL based approaches, excellent results are obtained using different architectures. The layers of the architecture are elegantly set to achieve satisfactory results. These methods require various parameters to be tuned, such as kernel size, number of layers, etc., resulting in a substantial computational cost. It is also tedious to obtain optimal values for many parameters. It is noted that systems required for CNN based approaches are highly configured with GPUs [84, 85]. In addition, such systems have a large memory requirement. In spite of the superior performance of the deep neural networks, they produce lower accuracies on negative images (i.e., semantic adversarial examples) [91]. The data resampling can be performed to balance the samples of normal and abnormal classes [92]. The structure used in [93-100,112] can be combined with a handcrafted feature learning approach to increase the robustness of the developed model.

As a summary, complete study is based on the categorization of the brain MRI images using holistic features. It is noted that the handcrafted feature approach exhibits promising results in handling both two - and multiclass categorization of the brain pathology. Methods such as VMD + bispectral features over graph embedding feature space have efficiently handled the minute anatomical variations in the brain images. It is also observed that entropy and textural

based feature extraction schemes are able to better detect pixel variations. These methodologies can be extended to build other CAD tools using fundus images [106,111], ultrasound images [107], thermograms [108], etc. However, CNN based approaches gave the ad hoc solution to BPI, rather than the generalized solution.

### *Open issues for future development*

Since BPI for all types of abnormalities is an open challenge for the research community, at this time it is difficult to determine whether existing methods are sufficient for the task at hand. However, for successful implementation of real-world BPI systems, it is suggested that investigators could focus on the following issues.

1. **Computing algorithms based on large dataset:** There is a need for publicly available datasets with large size and diversity in support of new studies. The research community should also create a public leaderboard website to submit new results. The computing algorithms should consider BPI as a multiclass classification problem, rather than as two-class. On the other hand, investigators should develop computing algorithms to handle uncertainties in the brain data. For which, designing of compact discriminative features to represent brain is the key requirement. In addition, to reduce the possibility of human error, the system should be robust to the handling of subtle variations in brain data. Thus a novel algorithm which uses the complementary advantages of handcrafted feature based and DL based methods is suggested to address the large scale BPI problem.
2. **Computing algorithms based on clinical requirements:** The computing algorithms need to work based upon two or three clinical guidelines. Furthermore, detecting the appropriate guidelines and mitigating conflicts are necessary. During which time, the complexity may increase in searching for a solution. Hence, a novel optimization technique is required to obtain a solution rapidly. At the same time, the process should be general enough so as to build a model using global clinical data for prediction of a particular disease. Therefore, medical doctors will be enabled to cross-verify their prescription with the predicted outcome. However, standardization analysis and collection of data from various sources will be interesting and challenging topics.



3. **Computing algorithms based on cloud platform:** There is a need for mobile application (App) which can be networked with medical doctors and their patients. Due to limited resource constraints including those of memory and processing speed, the App should utilize a cloud in order to execute computationally intensive algorithms. Thus, the system could then provide easy access to the on-demand healthcare mobile App and required data.

The required CAD model with suggested future requirements is shown in [Figure 11](#). Herewith, a patient may obtain feedback remotely from medical doctors and concomitant sophisticated computing algorithms. This could be rendered as a sustainable care component in future healthcare systems to improve patient quality-of-life at an early stage.

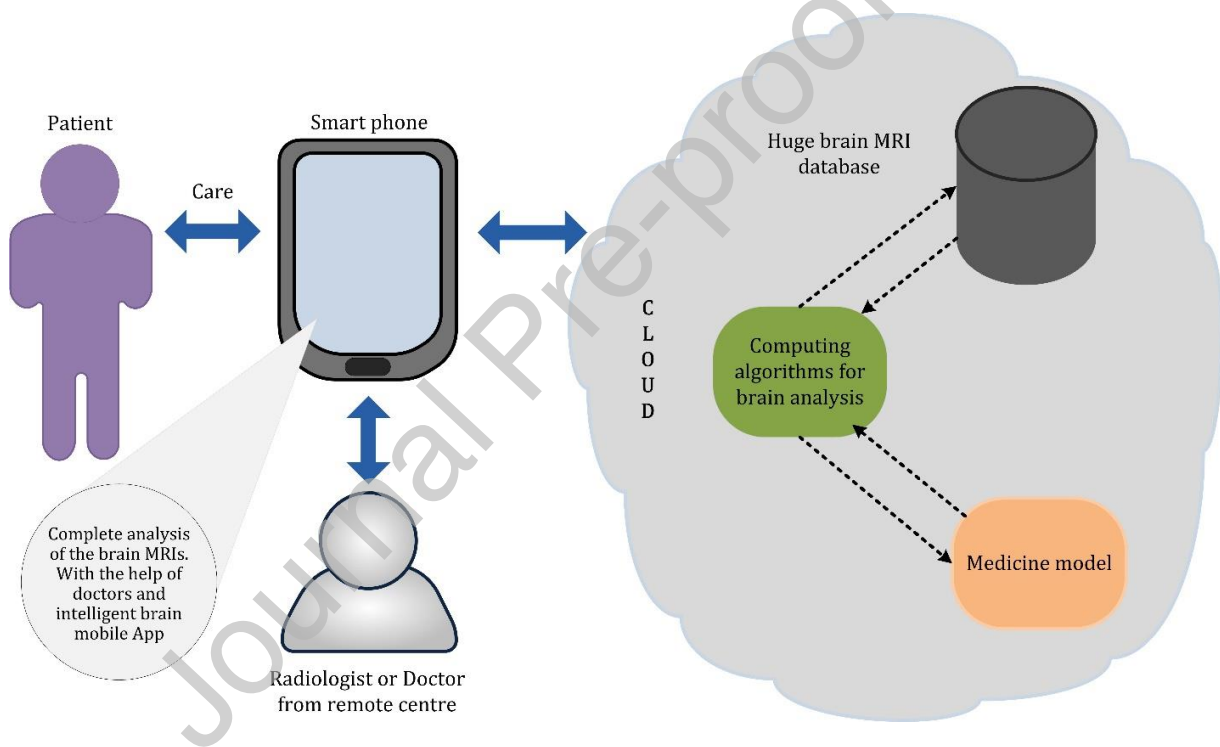


**Figure 11:** Advanced CAD model suggested for future implementation.

Moreover, CAD for BPI might even become predominant for diagnostics within the next few years, as it has several advantages:

- i. It identifies abnormal signs by comparing images so that a computerized analysis can be generated which will provide a secondary opinion.

- ii. Automation in decision making, extraction, and visualization of complex characteristics for the purpose of clinical diagnosis.
- iii. Mobile health services which facilitate doctor monitoring of patient health whenever required.
- iv. It can be used by a non-expert radiologist for fast analysis.
- v. Installation of this tool to rural area hospitals will increase the likelihood of early detection of fatal brain disease so that it may be cured.
- vi. It can be used as a learning device for practitioners in modern classroom teaching.

## 5. Conclusion

In this paper, we have presented an overview of state-of-the-art BPI systems. Over a period of time, many efforts have been made by investigators for the successful identification of brain pathology. Multiclass categorization of brain pathology using MRIs is still in its infancy. We have categorized the existing algorithms as handcrafted versus DL techniques, which were compared and reviewed. The contemporary algorithms have converged to solutions by achieving an identification accuracy of approximately 97% - 100%. However, at this time it is difficult to answer the question: are handcrafted techniques superior to CNN based techniques, or *vice versa*? In addition, we have addressed some research issues for future development, and suggest that it is a voracious time to further advance the topic of BPI.

## References

1. GBD 2015 Neurological Disorders Collaborator Group. Global, regional, and national burden of neurological disorders during 1990-2015: a systematic analysis for the Global Burden of Disease Study 2015. *The Lancet Neurology*. 2017 Nov;16(11):877–97.
2. Siuly S, Zhang Y. Medical Big Data: Neurological Diseases Diagnosis Through Medical Data Analysis. *Data Sci Eng*. Springer Berlin Heidelberg; 2016 Jul 27;1(2):54–64.
3. Hayward RM, Patronas N, Baker EH, Vézina G, Albert PS, Warren KE. Inter-observer variability in the measurement of diffuse intrinsic pontine gliomas. *J Neurooncol*. Springer US; 2008 Oct;90(1):57–61.
4. Chlebus G, Meine H, Thoduka S, Abolmaali N, van Ginneken B, Hahn HK, et al. Reducing inter-observer variability and interaction time of MR liver volumetry by combining automatic CNN-based liver segmentation and manual corrections. Punithakumar K, editor. *PLoS ONE*. Public Library of Science; 2019;14(5):e0217228.

5. Miller DD, Brown EW. Artificial Intelligence in Medical Practice: The Question to the Answer? The American Journal of Medicine. 2018 Feb;131(2):129–33.
6. Matheson R. Faster analysis of medical images [Internet]. MIT News. 2018 [cited 2019 Jun 19]. Available from: <http://news.mit.edu/2018/faster-analysis-of-medical-images-0618>
7. European Society of Radiology 2009. The future role of radiology in healthcare. Insights Imaging. Springer Berlin Heidelberg; 2010 Jan;1(1):2–11.
8. Zaharchuk G, Gong E, Wintermark M, Rubin D, Langlotz CP. Deep Learning in Neuroradiology. American Journal of Neuroradiology. American Journal of Neuroradiology; 2018 Oct 1;39(10):1776–84.
9. Jim Basilakis, H. Nigel Lovell, J. Stephen Redmond, G. Branko Celler, Design of a decision-support architecture for management of remotely monitored patients, IEEE Trans. Inf. Technol. Biomed. 14(5)(2010)1216–1226.
10. Fujita, H., Uchiyama, Y., Nakagawa, T., Fukuoka, D., Hatanaka, Y., Hara, T., et al. (2008). Computer-aided diagnosis: The emerging of three CAD systems induced by Japanese health care needs. Computer Methods and Programs in Biomedicine, 92(3), 238–248.
11. Latif, G., Kazmi, S. B., Jaffar, M. A., & Mirza, A. M. (2010). Classification and segmentation of brain tumor using texture analysis. In Proceedings of the (9th) 2010 WSEAS international conference on artificial intelligence knowledge engineering and data bases (pp. 147–155).
12. Shuihua Wang, Yin Zhang, Tianmin Zhan, Preetha Phillips, et al. Pathological Brain Detection by Artificial Intelligence in Magnetic Resonance Imaging Scanning, Progress In Electromagnetics Research, Vol. 156, 105–133, 2016
13. Di lin , Athanasios V. Vasilakos , YuTang , Yuanzhe Yao, Neural networks for computer-aided diagnosis in medicine: A review. Neurocomputing 216 (2016) 700–708
14. Wang SH., Zhang YD., Dong Z., Phillips P. (2018) Comparison of Artificial Intelligence–Based Pathological Brain Detection Systems. In: Pathological Brain Detection. Brain Informatics and Health. Springer, Singapore pp 179–190
15. Taleb-Ahmed A, Dubois P, Duquenois E. Analysis methods of CT-scan images for the characterization of the bone texture: First results. Pattern Recognition Letters. North-Holland; 2003 Aug 1;24(12):1971–82.
16. Currie S, Hoggard N, Craven IJ, Hadjivassiliou M, Wilkinson ID. Understanding MRI: basic MR physics for physicians. Postgrad Med J. The Fellowship of Postgraduate Medicine; 2013 Apr;89(1050):209–23.
17. Available in [https://www.nibib.nih.gov/science-education/science\\_topics/magnetic-resonance-imaging-mri](https://www.nibib.nih.gov/science-education/science_topics/magnetic-resonance-imaging-mri). Last accessed data 07/03/2019
18. D. Cireşan, U. Meier, J. Masci, and J. Schmidhuber, “A committee of neural networks for traffic sign classification,” in International Joint Conference on Neural Networks, San Jose, CA, 2011, pp. 1918–1921.
19. U Raghavendra, Hamido Fujita, Sulatha V Bhandary, Anjan Gudigar, Jen Hong Tan, U Rajendra Acharya, Deep convolution neural network for accurate diagnosis of glaucoma using digital fundus images, Information Sciences, Vol. 441, pp.41–49, 2018.
20. D. Jude Hemanth, C. Kezi Selva Vijila and J. Anitha , “Performance Improved PSO based Modified Counter Propagation Neural Network for Abnormal MR Brain Image Classification”, Int. J. Advance. Soft Comput. Appl., Vol. 2, No. 1, pp 65–84, March 2010

21. E. El-Dahshan, H. Mohsen, K. Revett and A. Salem, "Computer-aided diagnosis of human brain tumor through MRI: A survey and a new algorithm", *Expert Systems with Applications*, vol. 41, no. 11, pp. 5526-5545, 2014. Available: 10.1016/j.eswa.2014.01.021.
22. D. Jha and G. Kwon, "Development of an Efficient Cascade Pathological-Brain Detection System using a Median Filter and Quadratic Discriminant Analysis", *IEIE Transactions on Smart Processing & Computing*, vol. 7, no. 2, pp. 140-147, 2018. Available: 10.5573/ieiespc.2018.7.2.140.
23. D. Jha, J. Kim, M. Choi and G. Kwon, "Pathological Brain Detection Using Weiner Filtering, 2D-Discrete Wavelet Transform, Probabilistic PCA, and Random Subspace Ensemble Classifier", *Computational Intelligence and Neuroscience*, vol. 2017, pp. 1-11, 2017. Available: 10.1155/2017/4205141.
24. D. R. Nayak, R. Dash and B. Majhi, "An improved extreme learning machine for pathological brain detection," *TENCON 2017 - 2017 IEEE Region 10 Conference*, Penang, 2017, pp. 13-18. doi: 10.1109/TENCON.2017.822782
25. D. R. Nayak, R. Dash, Z. Lu, S. Lu and B. Majhi, "SCA-RELM: A New Regularized Extreme Learning Machine Based on Sine Cosine Algorithm for Automated Detection of Pathological Brain," *2018 27th IEEE International Symposium on Robot and Human Interactive Communication (RO-MAN)*, Nanjing, 2018, pp. 764-769. doi: 10.1109/ROMAN.2018.8525509
26. D. Nayak, R. Dash and B. Majhi, "Development of pathological brain detection system using Jaya optimized improved extreme learning machine and orthogonal ripplelet-II transform", *Multimedia Tools and Applications*, vol. 77, no. 17, pp. 22705-22733, 2018. Available: 10.1007/s11042-017-5281-x.
27. D. Nayak, R. Dash and B. Majhi, "Discrete ripplelet-II transform and modified PSO based improved evolutionary extreme learning machine for pathological brain detection", *Neurocomputing*, vol. 282, pp. 232-247, 2018. Available: 10.1016/j.neucom.2017.12.030.
28. D. Nayak, R. Dash and B. Majhi, "An Improved Pathological Brain Detection System Based on Two-Dimensional PCA and Evolutionary Extreme Learning Machine", *Journal of Medical Systems*, (2018) 42: 19. Available: 10.1007/s10916-017-0867-4.
29. Anjan Gudigar , U. Raghavendra , Tan Ru San , Edward J. Ciaccio ,U. Rajendra Acharya ,” Application of multiresolution analysis for automated detection of brain abnormality using MR images: A comparative study”, *Future Generation Computer Systems* 90 (2019) 359–367.
30. Lavneet Singh, Girija Chetty, and Dharmendra Sharma,” A Novel Machine Learning Approach for Detecting the Brain Abnormalities from MRI Structural Images”, *PRIB 2012, LNBI 7632*, pp. 94–105, 2012
31. Kinsler, J. M., & Johnson, J. L. (1996). Stabilized input with a feedback pulse-coupled neural network. *Optical Engineering*, 35(8), 2158–2161.
32. HebaMohsen, EI-Sayed Ahmed EI-Dahshan, Abdel-Badeeh M. Salem, “A Machine Learning Technique for MRI Brain Images”, *The 8th International Conference on INFOrmatics and Systems (INFOS2012)*, pp. 161-165, 2012
33. D. Nayak, R. Dash, B. Majhi and V. Prasad, "Automated pathological brain detection system: A fast discrete curvelet transform and probabilistic neural network based approach", *Expert Systems with Applications*, vol. 88, pp. 152-164, 2017. Available: 10.1016/j.eswa.2017.06.038.

34. S. Chaplot, L. Patnaik and N. Jagannathan, "Classification of magnetic resonance brain images using wavelets as input to support vector machine and neural network", *Biomedical Signal Processing and Control*, vol. 1, no. 1, pp. 86-92, 2006. Available: 10.1016/j.bspc.2006.05.002.
35. EL-SAYED A. EL-DAHSHAN, ABDEL-BADEEH M. SALEM, AND TAMER H. YOUNIS, " A Hybrid Technique For Automatic MRI Brain Images Classification", *STUDIA UNIV. BABES-BOLYAI, INFORMATICA*, Volume LIV, Number 1, pp 55-67, 2009
36. Y. Zhang, S. Wang and L. Wu, "A Novel Method For Magnetic Resonance Brain Image Classification Based On Adaptive Chaotic Pso", *Progress In Electromagnetics Research*, vol. 109, pp. 325-343, 2010. Available: 10.2528/pier10090105.
37. E. El-Dahshan, T. Hosny and A. Salem, "Hybrid intelligent techniques for MRI brain images classification", *Digital Signal Processing*, vol. 20, no. 2, pp. 433-441, 2010. Available: 10.1016/j.dsp.2009.07.002.
38. Y. Zhang, Z. Dong, L. Wu and S. Wang, "A hybrid method for MRI brain image classification", *Expert Systems with Applications*, vol. 38, no. 8, pp. 10049-10053, 2011. Available: 10.1016/j.eswa.2011.02.012
39. N. H. Rajini and R. Bhavani, "Classification of MRI brain images using k-nearest neighbor and artificial neural network," 2011 International Conference on Recent Trends in Information Technology (ICRTIT), Chennai, Tamil Nadu, 2011, pp. 863-868. doi: 10.1109/ICRTIT.2011.5972341
40. Y. Zhang, L. Wu and S. Wang, "Magnetic Resonance Brain Image Classification By An Improved Artificial Bee Colony Algorithm", *Progress In Electromagnetics Research*, vol. 116, pp. 65-79, 2011. Available: 10.2528/pier11031709.
41. Y. Zhang and L. Wu, "An Mr Brain Images Classifier Via Principal Component Analysis And Kernel Support Vector Machine", *Progress In Electromagnetics Research*, vol. 130, pp. 369-388, 2012. Available: 10.2528/pier12061410.
42. Y. Zhang, S. Wang, G. Ji and Z. Dong, "An MR Brain Images Classifier System via Particle Swarm Optimization and Kernel Support Vector Machine", *The Scientific World Journal*, vol. 2013, pp. 1-9, 2013. Available: 10.1155/2013/130134.
43. Y. Zhang, S. Wang, G. Ji and Z. Dong, "Genetic Pattern Search and Its Application to Brain Image Classification", *Mathematical Problems in Engineering*, vol. 2013, pp. 1-8, 2013. Available: 10.1155/2013/580876.
44. D. R. Nayak, R. Dash and B. Majhi, "Classification of brain MR images using discrete wavelet transform and random forests," 2015 Fifth National Conference on Computer Vision, Pattern Recognition, Image Processing and Graphics (NCVPRIPG), Patna, 2015, pp. 1-4.
45. D. Nayak, R. Dash and B. Majhi, "Brain MR image classification using two-dimensional discrete wavelet transform and AdaBoost with random forests", *Neurocomputing*, vol. 177, pp. 188-197, 2016. Available: 10.1016/j.neucom.2015.11.034.
46. Muhammad Faisal Siddiqui , Ghulam Mujtaba , Ahmed Wasif Reza and Liyana Shuib ,” Multi-Class Disease Classification in Brain MRIs Using a Computer-Aided Diagnostic System”, *Symmetry* 2017, 9, 37; doi:10.3390/sym9030037
47. U. Bagct and Li Bai, "A Comparison of Daubechies and Gabor Wavelets for Classification of MR Images," 2007 IEEE International Conference on Signal Processing and Communications, Dubai, 2007, pp. 676-679. doi: 10.1109/ICSPC.2007.4728409

48. S. Das, M. Chowdhury and M. Kundu, "Brain MR Image Classification Using Multiscale Geometric Analysis Of Ripplet", *Progress In Electromagnetics Research*, vol. 137, pp. 1-17, 2013. Available: 10.2528/pier13010105.
49. Y. Zhang, S. Chen, S. Wang, J. Yang and P. Phillips, "Magnetic resonance brain image classification based on weighted-type fractional Fourier transform and nonparallel support vector machine", *International Journal of Imaging Systems and Technology*, vol. 25, pp. 317-327, 2015. Available: 10.1002/ima.22144.
50. Y. Zhang et al., "Magnetic Resonance Brain Image Classification via Stationary Wavelet Transform and Generalized Eigenvalue Proximal Support Vector Machine", *Journal of Medical Imaging and Health Informatics*, vol. 5, no. 7, pp. 1395-1403, 2015. Available: 10.1166/jmih.2015.1542.
51. D. Nayak, R. Dash and B. Majhi, "Pathological brain detection using curvelet features and least squares SVM", *Multimed Tools Appl* (2018) 77:3833–3856
52. M. Maitra and A. Chatterjee, "A Slantlet transform based intelligent system for magnetic resonance brain image classification", *Biomedical Signal Processing and Control*, vol. 1, no. 4, pp. 299-306, 2006. Available: 10.1016/j.bspc.2006.12.001.
53. M. Maitra and A. Chatterjee, "Hybrid multiresolution Slantlet transform and fuzzy c-means clustering approach for normal-pathological brain MR image segregation", *Medical Engineering & Physics*, vol. 30, no. 5, pp. 615-623, 2008. Available: 10.1016/j.medengphy.2007.06.009.
54. R. M. Haralick, K. Shanmugam and I. Dinstein, "Textural Features for Image Classification," in *IEEE Transactions on Systems, Man, and Cybernetics*, vol. SMC-3, no. 6, pp. 610-621, Nov. 1973.
55. Sahar Jafarpour, Zahra Sedghi, Mehdi Chehel Amirani, "A Robust Brain MRI Classification with GLCM Features", *International Journal of Computer Applications*, volume 37– No.12, pp. 1-5, January 2012
56. Kale, V.V., Hamde, S.T. & Holambe, R.S. "Multi class disorder detection of magnetic resonance brain images using composite features and neural network" *Biomed. Eng. Lett.* (2019). <https://doi.org/10.1007/s13534-019-00103-1>
57. H. Kalbkhani, M. Shayesteh and B. Zali-Vargahan, "Robust algorithm for brain magnetic resonance image (MRI) classification based on GARCH variances series", *Biomedical Signal Processing and Control*, vol. 8, no. 6, pp. 909-919, 2013. Available: 10.1016/j.bspc.2013.09.001.
58. M. Saritha, K. Paul Joseph and A. Mathew, "Classification of MRI brain images using combined wavelet entropy based spider web plots and probabilistic neural network", *Pattern Recognition Letters*, vol. 34, no. 16, pp. 2151-2156, 2013. Available: 10.1016/j.patrec.2013.08.017.
59. Y. Zhang, S. Wang, P. Phillips, Z. Dong, G. Ji and J. Yang, "Detection of Alzheimer's disease and mild cognitive impairment based on structural volumetric MR images using 3D-DWT and WTA-KSVM trained by PSOTVAC", *Biomedical Signal Processing and Control*, vol. 21, pp. 58-73, 2015. Available: 10.1016/j.bspc.2015.05.014.
60. Y. Zhang, S. Wang, P. Sun and P. Phillips, "Pathological brain detection based on wavelet entropy and Hu moment invariants", *Bio-Medical Materials and Engineering*, vol. 26, no. 1, pp. S1283-S1290, 2015. Available: 10.3233/bme-151426
61. Y. Zhang et al., "Pathological brain detection in MRI scanning by wavelet packet Tsallis entropy and fuzzy support vector machine", *SpringerPlus*, vol. 4, no. 1, 2015. Available: 10.1186/s40064-015-1523-4 [Accessed 9 March 2019].

62. Y. Zhang, Z. Dong, S. Wang, G. Ji and J. Yang, "Preclinical Diagnosis of Magnetic Resonance (MR) Brain Images via Discrete Wavelet Packet Transform with Tsallis Entropy and Generalized Eigenvalue Proximal Support Vector Machine (GEPSVM)", *Entropy*, vol. 17, no. 4, pp. 1795-1813, 2015. Available: 10.3390/e17041795.
63. S. Wang et al., "Pathological Brain Detection by a Novel Image Feature—Fractional Fourier Entropy", *Entropy*, vol. 17, no. 12, pp. 8278-8296, 2015. Available: 10.3390/e17127877.
64. Y. Zhang, Y. Sun, P. Phillips, G. Liu, X. Zhou and S. Wang, "A Multilayer Perceptron Based Smart Pathological Brain Detection System by Fractional Fourier Entropy", *Journal of Medical Systems*, vol. 40, no. 7, 2016. Available: 10.1007/s10916-016-0525-2.
65. S. Wang, S. Lu, Z. Dong, J. Yang, M. Yang and Y. Zhang, "Dual-Tree Complex Wavelet Transform and Twin Support Vector Machine for Pathological Brain Detection", *Applied Sciences*, (2016), 6, 169, pp.1-18
66. Y. Zhang et al., "Fractal Dimension Estimation for Developing Pathological Brain Detection System Based on Minkowski-Bouligand Method," in *IEEE Access*, vol. 4, pp. 5937-5947, 2016.
67. D. Nayak, R. Dash, X. Chang, B. Majhi and S. Bakshi, "Automated Diagnosis of Pathological Brain Using Fast Curvelet Entropy Features", *IEEE Transactions on Sustainable Computing*, pp. 1-1, 2018. Available: 10.1109/tsusc.2018.2883822.
68. A. Gudigar, U. Raghavendra, E. J. Ciaccio, N. Arunkumar, E. Abdulhay and U. R. Acharya, "Automated Categorization of Multi-Class Brain Abnormalities Using Decomposition Techniques With MRI Images: A Comparative Study," in *IEEE Access*, vol. 7, pp. 28498-28509, 2019.
69. Y. Zhang et al., "Detection of subjects and brain regions related to Alzheimer's disease using 3D MRI scans based on eigenbrain and machine learning", *Frontiers in Computational Neuroscience*, vol. 9, 2015. Available: 10.3389/fncom.2015.00066.
70. T. Li, W. Li, Y. Yang and W. Zhang, "Classification of brain disease in magnetic resonance images using two-stage local feature fusion", *PLOS ONE*, vol. 12, no. 2, p. e0171749, 2017. Available: 10.1371/journal.pone.0171749.
71. Y. Zhang, Y. Jiang, W. Zhu, S. Lu and G. Zhao, "Exploring a smart pathological brain detection method on pseudo Zernike moment", *Multimedia Tools and Applications*, vol. 77, no. 17, pp. 22589-22604, 2017. Available: 10.1007/s11042-017-4703-0
72. P. N. Belhumeur, J. P. Hespanha, and D. J. Kriegman (1997) Eigenfaces vs. fisherfaces: Recognition using class specific linear projection. *IEEE Trans. Pattern Anal. Mach. Intell.* 19(7): 711–720
73. I. Guyon and A. Elisseeff (2003) An introduction to variable and feature selection. *J. Mach. Learn. Res.* 3: 1157–1182
74. S. Lahmiri and M. Boukadoum, "Brain MRI classification using an ensemble system and LH and HL wavelet sub-bands features," 2011 IEEE Third International Workshop On Computational Intelligence In Medical Imaging, Paris, 2011, pp. 1-7.
75. S. Yan, D. Xu, B. Zhang, H.-J. Zhang, Q. Yang, and S. Lin (2007) Graph embedding and extensions: A general framework for dimensionality reduction. *IEEE Transactions on Pattern Analysis and Machine Intelligence* 29(1):40-51
76. Luis Javier Herrera, Ignacio Rojas, H. Pomares, A. Guillén, O. Valenzuela, O. Baños," Classification of MRI images for Alzheimer's disease detection", *SocialCom/PASSAT/BigData/EconCom/BioMedCom 2013* 846- 851

77. O. Sahu, V. Anand, V. Kanhangad and R. Pachori, "Classification of magnetic resonance brain images using bi-dimensional empirical mode decomposition and autoregressive model", *Biomedical Engineering Letters*, vol. 5, no. 4, pp. 311-320, 2015. Available: 10.1007/s13534-015-0208-9.
78. Breiman, L. Random forests. *Mach. Learn.* **2001**, 45, 5–32.
79. G.-B. Huang, Q.-Y. Zhu, and C.-K. Siew, "Extreme learning machine: theory and applications," *Neurocomputing*, vol. 70, no. 1, pp. 489–501, 2006, doi: 10.1016/j.neucom.2005.12.126.
80. Hagan M, Demuth HB, Beale MH, De Jess O. *Neural network design*. 2nd ed. Boston: PWS Publishing; 1996.
81. C. Burges, A tutorial on support vector machines for pattern recognition, *Data Mining Knowl. Discov.* 2 (1998) 121–167, doi: 10.1023/a:1009715923555
82. Yang, G., Zhang, Y., Yang, J. et al. Automated classification of brain images using wavelet-energy and biogeography-based optimization, *Multimed Tools Appl* (2016) 75: 15601–15617 Volume 75, Issue 23. <https://doi.org/10.1007/s11042-015-2649-7>
83. Y. Zhang et al., "Preliminary research on abnormal brain detection by wavelet-energy and quantum-behaved PSO", *Technology and Health Care*, vol. 24, no. 2, pp. S641-S649, 2016. Available: 10.3233/thc-161191.
84. Siyuan Lu, Zhihai Lu, Yu-Dong Zhang, "Pathological brain detection based on AlexNet and transfer learning", *Journal of Computational Science* 30 (2019) 41–47
85. Muhammed Talo , Ulas Baran Baloglu , Ozal Yildirima, U Rajendra Acharya,"Application of deep transfer learning for automated brain abnormality classification using MR images," *Cognitive Systems Research*, Volume 54, May 2019, Pages 176-188
86. S. Lu, Z. Lu, J. Yang, M. Yang and S. Wang, "A pathological brain detection system based on kernel based ELM", *Multimedia Tools and Applications*, vol. 77, no. 3, pp. 3715-3728, 2018. Available: 10.1007/s11042-016-3559-z.
87. Xingxing Zhou, Shuihua Wang, Wei Xu, Genlin Ji, Preetha Phillips, Ping Sun, and Yudong Zhang, "Detection of Pathological Brain in MRI Scanning Based on Wavelet-Entropy and Naive Bayes Classifier", *IWBBIO 2015, Part I, LNCS 9043*, pp. 201–209, 2015.
88. S. Lahmiri and M. Boukadoum, "Automatic brain MR images diagnosis based on edge fractal dimension and spectral energy signature," 2012 Annual International Conference of the IEEE Engineering in Medicine and Biology Society, San Diego, CA, 2012, pp. 6243-6246. doi: 10.1109/EMBC.2012.6347421
89. T.R. Sivapriya, V. Saravanan, and P. Ranjit Jeba Thangaiah," Texture Analysis of Brain MRI and Classification with BPN for the Diagnosis of Dementia", *CCSEIT 2011, CCIS 204*, pp. 553–563, 2011.
90. M. F. Bin Othman, N. Abdullah and N. A. B. A. Rusli, "An overview of MRI brain classification using FPGA implementation," 2010 IEEE Symposium on Industrial Electronics and Applications (ISIEA), Penang, 2010, pp. 623-628. doi: 10.1109/ISIEA.2010.5679389
91. H. Hosseini and R. Poovendran, "Deep neural networks do not recognize negative images," *CoRR*, vol. abs/1703.06857, 2017. [Online]. Available: <http://arxiv.org/abs/1703.06857>
92. He H, Yang B, Garcia EA, Li S ADASYN: adaptive synthetic sampling approach for imbalanced learning, *Proceedings of the International Joint Conference on Neural Networks, {IJCNN} 2008*, part of the IEEE World Congress on Computational Intelligence, {WCCI} 2008, Hong Kong, China, pp 1–6



93. U Raghavendra, N Shyamasunder Bhat, Anjan Gudigar, U Rajendra Acharya, Automated system for the detection of thoracolumbar fracture using a CNN architecture, *Future Generation Computer Systems*, Vol. 85, pp. 184-189, 2018
94. U Raghavendra, Hamido Fujita, Sulatha V Bhandary, Anjan Gudigar, Jen Hong Tan, U Rajendra Acharya, Deep convolution neural network for accurate diagnosis of glaucoma using digital fundus images, *Information Sciences*, Vol. 441, pp.41-49, 2018.
95. U. Rajendra Acharya, Shu Lih Oh, Yuki Hagiwara, Jen Hong Tan, Hojjat Adeli, D. P Subha, Automated EEG-based screening of depression using deep convolutional neural network, *Computer Methods and Programs in Biomedicine*, Volume 161, 2018, Pages 103-113.
96. Jen Hong Tan, Sulatha V Bhandary, Sobha Sivaprasad, Yuki Hagiwara, Akanksha Bagchi, U Raghavendra, A Krishna Rao, Biju Raju, Nitin Shridhara Shetty, Arkadiusz Gertych, Kuang Chua Chua, U Rajendra Acharya, Age-related Macular Degeneration detection using deep convolutional neural network, *Future Generation Computer Systems*, Vol. 8, pp. 127-135, 2018.
97. U Rajendra Acharya, Shu Lih Oh, Yuki Hagiwara, Jen Hong Tan, Muhammad Adam, Arkadiusz Gertych, Ru San Tan, A deep convolutional neural network model to classify heartbeats, *Computers in biology and medicine*, Vol. 89, pp. 389-396, 2017.
98. Jen Hong Tan, Yuki Hagiwara, Winnie Pang, Ivy Lim, Shu Lih Oh, Muhammad Adam, Ru San Tan, Ming Chen, U Rajendra Acharya, Application of stacked convolutional and long short-term memory network for accurate identification of CAD ECG signals, *Computers in biology and medicine*, Vol. 94, pp. 19-26, 2018
99. U. Rajendra Acharya, Hamido Fujita, Shu Lih Oh, U. Raghavendra, Jen Hong Tan, Muhammad Adam, Arkadiusz Gertych, Yuki Hagiwara, Automated identification of shockable and non-shockable life-threatening ventricular arrhythmias using convolutional neural network, *Future Generation Computer Systems*, Volume 79, Part 3, 2018, Pages 952-959.
100. Oh SL, Vinesh J, Ciaccio EJ, Yuvaraj R, Acharya UR. Deep Convolutional Neural Network Model for Automated Diagnosis of Schizophrenia Using EEG Signals. *Applied Sciences* 2019;9:2870
101. C. Baur, B. Wiestler, S. Albarqouni, N. Navab, Deep autoencoding models for unsupervised anomaly segmentation in brain MR images, *Brainlesion: Glioma, Multiple Sclerosis, Stroke and Traumatic Brain Injuries*, 2019, Cham, pp 161—169
102. U. Raghavendra, Anjan Gudigar, Sulatha V. Bhandary, Tejaswi N. Rao, Edward J. Ciaccio, U. Rajendra Acharya, A Two Layer Sparse Autoencoder for Glaucoma Identification with Fundus Images, *Journal of Medical Systems* (2019) 43:299
103. Lirong Chen , Qingfeng Guan , Bin Feng , Hanqiu Yue , Junyi Wang and Fan Zhang, A Multi-Convolutional Autoencoder Approach to Multivariate Geochemical Anomaly Recognition, *Minerals* 2019, 9, 270; doi:10.3390/min9050270
104. Hans E. Atlason, Askell Love M.D., Sigurdur Sigurdsson, Vilmundur Gudnason M.D., and Lotta M. Ellingsen "Unsupervised brain lesion segmentation from MRI using a convolutional autoencoder", *Proc. SPIE 10949, Medical Imaging 2019: Image Processing*, 109491H
105. Vandana V. Kale, Satish T. Hamde, Raghunath S. Holambe, Brain disease diagnosis using local binary pattern and steerable pyramid, *Int J Multimed Info Retr* (2019) 8: 155. <https://doi.org/10.1007/s13735-019-00174-x>
106. U. Raghavendra, Sulatha V. Bhandary, Anjan Gudigar, U. Rajendra Acharya, Novel expert system for glaucoma identification using non-parametric spatial envelope energy spectrum with fundus images, *Biocybernetics and Biomedical Engineering*, Volume 38 (2018) 170 – 180.

107. Filippo Molinari, U. Raghavendra, Anjan Gudigar, Kristen M. Meiburger, U. Rajendra Acharya, An efficient data mining framework for the characterization of symptomatic and asymptomatic carotid plaque using bidimensional empirical mode decomposition technique, *Medical & Biological Engineering & Computing* (2018) 56:1579–1593
108. U Raghavendra, Anjan Gudigar, Tejaswi N Rao, Edward J Ciaccio, E.Y.K. Ng, U. Rajendra Acharya, Computer aided diagnosis for the identification of breast cancer using thermogram images: A comprehensive review, *Infrared Physics & Technology*, 2019, 103041.
109. Deepak Ranjan Nayak, Ratnakar Dash, Banshidhar Majhi, U. Rajendra Acharya, Application of fast curvelet Tsallis entropy and kernel random vector functional link network for automated detection of multiclass brain abnormalities, *Computerized Medical Imaging and Graphics*, 77, 2019, 101656.
110. Muhammed Talo, Ozal Yildirim, Ulas Baran Baloglu, Galip Aydin, U Rajendra Acharya, Convolutional neural networks for multi-class brain disease detection using MRI images, *Computerized Medical Imaging and Graphics*, 2019.
111. S. Maheshwari, R. B. Pachori and U. R. Acharya, Automated Diagnosis of Glaucoma Using Empirical Wavelet Transform and Correntropy Features Extracted From Fundus Images, *IEEE Journal of Biomedical and Health Informatics*, vol. 21, no. 3, pp. 803-813, 2017.
112. Oh, S.L., Hagiwara, Y., Raghavendra, U. et al. A deep learning approach for Parkinson's disease diagnosis from EEG signals, *Neural Comput & Applic* (2018). <https://doi.org/10.1007/s00521-018-3689-5>
113. U. Rajendra Acharya, Steven Lawrence Fernandes, Joel En WeiKoh, Edward J. Ciaccio, Mohd Kamil Mohd Fabell, U. John Tanik, V. Rajinikanth, Chai Hong Yeong, Automated Detection of Alzheimer's Disease Using Brain MRI Images– A Study with Various Feature Extraction Techniques, *Journal of Medical Systems*, 43: 302, 2019.

### **Conflict of interest**

The authors declare that they have no conflict of interest.